Medical Engineering and Physics 58 (2018) 56–63

Contents lists available at ScienceDirect

Medical Engineering and Physics

journal homepage: www.elsevier.com/locate/medengphy

Kinematics-based prediction of trunk muscle activity in response to multi-directional perturbations during sitting

Jacques Bobet[a], Kei Masani[b,c], Milos R. Popovic[b,c], Albert H. Vette[a,d,*]

[a] Department of Mechanical Engineering, University of Alberta, Donadeo Innovation Centre for Engineering, 9211 116 Street NW, Edmonton, Alberta T6G 1H9, Canada
[b] Rehabilitation Engineering Laboratory, Institute of Biomaterials and Biomedical Engineering, University of Toronto, 164 College Street, Toronto, Ontario M5S 3G9, Canada
[c] Rehabilitation Engineering Laboratory, Lyndhurst Centre, Toronto Rehabilitation Institute – University Health Network, 520 Sutherland Drive, Toronto, Ontario M4G 3V9, Canada
[d] Glenrose Rehabilitation Hospital, Alberta Health Services, 10230 111 Avenue NW, Edmonton, Alberta T5G 0B7, Canada

ARTICLE INFO

Article history:
Received 23 November 2017
Revised 7 May 2018
Accepted 28 May 2018

Keywords:
Electromyography
Functional electrical stimulation
Kinematics
Model prediction
Postural control
Seated balance

ABSTRACT

Recent work suggests that functional electrical stimulation can be used to enhance dynamic trunk stability following spinal cord injury. In this context, knowledge of the relation between trunk kinematics and muscle activation in non-disabled individuals may assist in developing kinematics-based neuroprostheses. Our objective was therefore to predict the activation profiles of the major trunk muscles from trunk kinematics following multi-directional perturbations during sitting. Trunk motion and electromyograms (EMG) from ten major trunk muscles were acquired in twelve non-disabled, seated individuals who experienced a force of approximately 200 N applied to the trunk in eight horizontal directions. A linear, time-invariant model with feedback gains on angular trunk displacement, velocity, and acceleration was optimized to predict the EMG from trunk kinematics. For each muscle, only the three directions that produced the largest EMG response were considered. Our results indicate that the time course of the processed EMG was similar across muscles and directions and that the model accounted for 68–92% of the EMG variance. A combination of neural and biomechanical mechanisms associated with trunk control can explain the obtained model parameters. Future work will apply the gained insights in the design of movement-controlled neuroprostheses for facilitating trunk stability following spinal cord injury.

1. Introduction

When balance of a seated person is challenged, postural stability is restored via activation of the major trunk muscles. Insights regarding the timing, amplitude, and time course of such muscular activation are thought to be important in various domains, including basic movement science, ergonomics, prevention, rehabilitation, and assistive technology development. In spite of this importance, the muscular response to seated perturbations and its characteristics are not fully understood or described.

It is well established that trunk muscle activity during perturbed sitting is needed for body stabilization [1,2], supporting the contributions of passive mechanisms such as spinal stiffness [3–5], viscoelastic properties of the trunk [6,7], and intraabdominal pressure [7,8]. Even during quiet sitting, *tonic muscle activity* can be observed in all major trunk muscles [2,9], with larger normalized electromyograms (EMG) occurring in the back extensors. Tonic muscle activity is, however, not sufficient to resist perturbations; therefore, the central nervous system (CNS) generates additional *phasic muscle activity* to brake outward motion of the trunk and bring it back to vertical. The phasic EMG levels are symmetric across body sides [2] and vary with the postural perturbation direction. Furthermore, each trunk muscle responds to multiple, but not all perturbation directions [2,9,10].

A number of theories have been advanced to explain and model the EMG response, but none of them allow quantitative predictions. McGill et al. [11] have proposed that one major role of trunk muscle activation is to keep the trunk from buckling under load. This theory, while broadly accepted in the field, does not allow for specific EMG time course predictions. Masani et al. [2] modeled, for each major trunk muscle separately, the relation between trunk displacement direction and peak EMG amplitude. In addition,

* Corresponding author. Neuromuscular Control & Biomechanics Laboratory, Department of Mechanical Engineering, University of Alberta, 10-203 Donadeo Innovation Centre for Engineering, 9211 116 Street NW, Edmonton, Alberta T6G 1H9, Canada
E-mail address: albert.vette@ualberta.ca (A.H. Vette).

https://doi.org/10.1016/j.medengphy.2018.05.004
1350-4533/

Milosevic et al. [12] used a self-organizing map to show that EMG amplitudes are clustered into certain patterns. However, their map only dealt with peak amplitudes and not the overall time course of respective EMG signals. Stokes and Gardner-Morse [13] attempted to predict muscle activation levels using various optimization schemes, but did so only for static loading conditions. While Goodworth and Peterka [14,15] have proposed a model that attributes the perturbation response to different neural circuits acting in parallel, it only predicts trunk torques and not the underlying muscle activity. Thus, no work to date exists to our knowledge that can predict the activation time course, or profile, of the major trunk muscles in response to multi-directional perturbations.

One area where an understanding of these activation profiles would be of benefit is in the use of functional electrical stimulation (FES) for enhancing trunk stability after spinal cord injury (SCI) [16–19]. FES has already been demonstrated to improve functional reach area, spinal alignment, pelvic orientation, pulmonary function, and the force that can be exerted with the hands [20,21]. In addition, both model simulations [22,23] and experimental studies [16,18–21,24,25] have shown that FES can improve dynamic sitting stability. Vanoncini et al. [16] used a simple, kinematics-based feedback controller to predict the trunk moments required for stabilizing an individual with SCI in the sagittal plane. Audu et al. [19] and Murphy et al. [25] delivered, using trunk acceleration as feedback, threshold-based FES to the hip and back extensors to stabilize seated individuals with SCI in the sagittal plane. Patel et al. (2017), using support surface perturbations applied to non-disabled individuals sitting in a wheelchair, found that feed-forward FES producing directionally-dependent muscle contractions was more effective in stabilizing the trunk in the sagittal plane than that producing co-contractions [24]. While these efforts suggest that physiologically timed muscle activations represent a promising FES control paradigm in the sagittal plane, it is not known how to best deliver such directionally-dependent stimulation across muscles for trunk movement in both the sagittal and frontal planes. One approach is to apply a kinematics-based, closed-loop stimulation strategy that is founded on trunk muscle activation profiles of non-disabled individuals responding to multi-directional trunk displacements.

Motivated by the described limitations in our theoretical and practical knowledge, the objective of this study was to provide a kinematics-based characterization and prediction of the EMG response of the major trunk muscles following multi-directional perturbations of seated balance. The prediction, which can be used for phasic, kinematics-based FES control, is built upon the hypothesis that the EMG response will correlate with the kinematics of the trunk during its displacements.

2. Methods

In this study, perturbation, EMG, and motion capture marker data collected in a previous experiment were used. While this dataset has been analyzed for different purposes [2,12,26], a brief description of the underlying experimental procedures is provided here.

2.1. Participants

Twelve healthy young men (age: 29 ± 7.7 years; height: 177 ± 4.7 cm; weight: 70.5 ± 9.6 kg; mean ± standard deviation) with no medical history or signs of neurological disorders were recruited. They gave written informed consent to participate in the study, the experimental procedures having been approved beforehand by the research ethics boards of the University of Toronto (Study ID: #15699) and the Toronto Rehabilitation Institute (Study ID: #05-017).

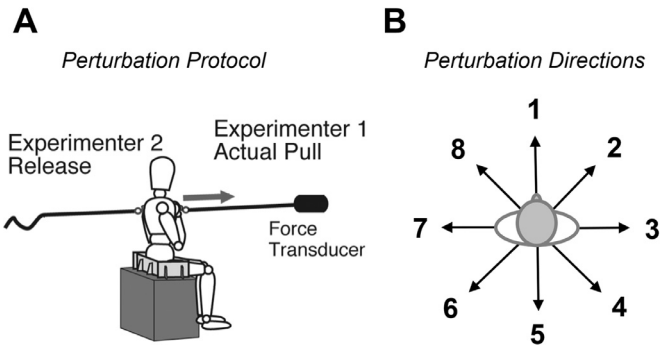

Fig. 1. Schematic of the experimental setup. (A) Two researchers cocked two ropes in two different directions. One of the two ropes, which also included a force transducer, was used for the actual perturbation. The purpose of cocking another rope in a different direction was to prevent the participant from anticipating the perturbation direction. The same researcher performed all perturbations to maintain consistency in perturbation force [2]. (B) The perturbation force was manually applied in eight different directions.

2.2. Experimental procedure

Surface EMG was collected using two AMT-8 EMG systems (Bortec Biomedical Ltd, Calgary, Canada). Each channel had a total gain of 2,000, a frequency response of 10–1,000 Hz, and a common-mode rejection ratio of 115 dB. Disposable silver-silver chloride electrodes, in a bipolar configuration 18 mm apart, were placed over the following muscles on both sides of the body: rectus abdominis (RA; vertically aligned 3 cm lateral of the umbilicus), external obliques (EO; aligned 45° off vertical, 15 cm lateral of the umbilicus), internal obliques (IO; aligned 45° off vertical, midway between the anterior superior iliac spine and the symphysis pubis, over the inguinal ligament), thoracic erector spinae (T9; aligned vertically, 5 cm lateral of the ninth thoracic spinous process), and lumbar erector spinae (L3: aligned vertically, 3 cm lateral of the third lumbar spinous process).

Horizontal perturbations were applied manually by one experimenter, using a rope attached to a belt around the chest just below the axillae (Fig. 1A). Perturbations were directed in eight different directions, at angles of 0°, 45°, 90°, 135°, 180°, 225°, 270°, and 315° (Fig. 1B). We refer to these as directions 1 to 8, with 1 being forward (0°), 3 being to the participant's right (90°), etc (Fig. 1B). A force sensor in series with the rope (MLP-100-CO–C, Transducer Techniques, Temecula, CA, USA; Amplifier: Model 9243, Burster, Germany) recorded the force of the perturbation (Fig. 1A). Force and EMG data were acquired synchronously at 2,000 Hz with a 64-channel, 12-bit analog-to-digital converter (NI6071E, National Instruments, Austin, USA) and custom data acquisition software embedded in LabView (National Instruments). The mechanical perturbation had an approximately triangular time course, with an average peak of 187 ± 31 N and an average half-width of 205 ± 26 ms. The motion, in three dimensions, of 19 markers placed on the trunk and head were collected at 100 Hz using an Optotrak 3020 motion analysis system (Northern Digital, Waterloo, Canada). For the present study, only the movement of the markers over the spinous processes of the sixth cervical (CV6) and third lumbar (LV3) vertebrae were used.

Participants sat on a hard, level surface with their eyes closed, hips and knees flexed to 90°, lower legs unsupported, and arms crossed. They were told to sit up tall and keep the neck and shoulders relaxed while listening to nature sounds through headphones to reduce auditory cues. The same experimenter delivered five perturbations in each of the eight directions (Fig. 1), with the order and timing of the perturbations being randomized. A rest was provided every 10 trials.

2.3. Experimental data processing

The EMG time series were band-pass filtered at 10–500 Hz with a zero-lag, second-order Butterworth filter. The full-wave rectified EMG signals were then smoothed using a zero-lag, second-order Butterworth low-pass filter with a cut-off frequency of 2.5 Hz and resampled at 100 Hz to match the kinematic data. The onset of the mechanical perturbation ("perturbation onset") was defined as the time at which the first time derivative of the perturbation force exceeded 12 N/s [2]. This point was set as time = 0 s for a given trial, and only data within the interval from 1 s before to 3 s following perturbation onset were retained.

All analyses were performed on 5-trial averages (hereafter called "ensembles"), rather than on individual trials. To generate these ensembles, EMG and kinematic data from all five trials for a given participant, perturbation direction, and muscle were first aligned via the perturbation onset and then averaged. For the ensembles, we then determined the time between the perturbation onset and the onset of the EMG response ("EMG onset time"). This onset was defined as the first EMG value exceeding the mean EMG activity plus three standard deviations during the one-second period preceding the perturbation onset. The time elapsed between the perturbation onset and the onset of the angular velocity of the trunk when moving away from equilibrium ("velocity onset time") was determined in the same manner.

From here on, the data processing methods differ from those of the previous studies using the dataset [2,12,26]. To apply a single-input, single-output model for predicting the EMG from trunk angle and its derivatives (*see below*), it was necessary to obtain a single variable representing trunk angle that could be used for all perturbation directions. Therefore, trunk angle was defined as the tilt angle, from the vertical, of the spine using a vector connecting the LV3 and CV6 markers. This is analogous to considering the trunk as a rigid inverted pendulum which is constrained to travel only in the plane that contains the perturbation force vector. While this does not capture the full complexity of trunk motion, it will be shown below that it is sufficient for predicting the EMG response. Trunk angle at time = 0 s was similar across ensembles, and was subtracted from the trunk angle time series so that the starting trunk angle for each ensemble was assumed to be zero. Trunk angle was filtered with a zero-lag, second-order Butterworth low-pass filter with a cut-off frequency of 10 Hz and differentiated twice to obtain angular trunk velocity and acceleration. Trunk velocity was obtained by taking the difference between consecutive values in the filtered trunk angle time series (function *diff* in Matlab; MathWorks, Natick, MA, USA) and multiplying it by the sampling frequency, 100 Hz ("one-point differentiation"). Trunk acceleration was obtained in the same manner, but using the trunk velocity instead of the trunk angle time series as the input. All calculations were performed in double precision with 64-bit accuracy. We refer to motion away from upright as "outward", and motion toward upright as "inward".

2.4. Prediction model

Our hypothesis was that, for each muscle, participant, and perturbation direction, the rectified, low-pass filtered EMG could be predicted from:

$$E(t) = G \cdot (K_P \cdot \theta(t) + K_D \cdot \omega(t) + K_A \cdot \alpha(t)) \quad (1)$$

where E is the difference between the EMG and its baseline level prior to perturbation onset (mV), t time (s), G a participant-specific scale factor for each muscle and participant (unitless), θ the trunk angle (rad), ω the angular trunk velocity (rad/s), α the angular trunk acceleration (rad/s^2), K_P the gain for amplifying trunk angle (proportional gain, mV/rad), K_D the gain for amplifying angular trunk velocity (derivative gain, mV·s/rad), and K_A the gain for amplifying angular trunk acceleration (acceleration gain, mV·s^2/rad). The G term was included to account for differences in absolute EMG levels between muscles and participants (due to factors such as muscle mass and skin impedance) and was assumed to be independent of perturbation direction. The other parameters were assumed to be constant within an ensemble, but could vary with muscle, participant, and perturbation direction. For the kinematic variables, outward motion was considered positive. We initially included a time delay in Eq. (1); however, since the optimization (*see below*) consistently set its value to zero, it was omitted.

The parameters in Eq. (1) cannot be uniquely determined; therefore, it was rewritten prior to parameter identification using:

$$E(t) = A \cdot \theta(t) + B \cdot \omega(t) + C \cdot \alpha(t) \quad (2)$$

where $A = G{\cdot}K_P$, $B = G{\cdot}K_D$, and $C = G{\cdot}K_A$ for each muscle, participant, and perturbation direction, with A, B, and C being constrained to be greater than zero [27]. We then identified, for each ensemble, the values of A, B, and C that minimized the fitting error using the function *fmincon* in Matlab [27]. Note that the variable minimized by *fmincon* was the sum of the squared error between the measured and predicted EMG. The goodness of fit was quantified using the coefficient of determination, R^2 [28]:

$$R^2 = 1 - \frac{SS_{res}}{SS_{tot}} \quad (3)$$

where SS_{res} is the sum of squared error between the measured and predicted EMG, and SS_{tot} the sum of squared deviations of the measured EMG from its mean.

Because A, B, and C depend on the participant-specific constant G, they are not directly comparable between participants. To allow between-participant and between-muscle comparisons, two ratios, r_D and r_A, were computed:

$$r_D = \frac{B}{A} = \frac{G \cdot K_D}{G \cdot K_P} = \frac{K_D}{K_P} \quad (4)$$

and

$$r_A = \frac{C}{A} = \frac{G \cdot K_A}{G \cdot K_P} = \frac{K_A}{K_P} \quad (5)$$

Because the participant-specific gain G appears in both the numerator and denominator of the ratios, it does not influence the ratios. As such, they can be compared across participants without normalizing the EMG amplitudes.

We refer to Eq. (1) as the *PDA model* as it contains proportional, derivative, and acceleration terms. We also fitted a model without the acceleration term to the same experimental data (*PD model*) for comparison.

2.5. Model validation

To validate the model, the best-fitting parameter values from the muscles of the right body side were used to predict the EMG of the muscles of the left body side. This was done for matching participants and directions. For example, the EMG from the left RA of participant 1 and direction 6 was predicted using the parameters from the right RA of participant 1 and direction 4. In this validation, we fixed the K_P, K_D, and K_A gains for a given muscle (Eq. (1)) to the values from the right side and varied G until the best possible fit with Eq. (2) was obtained. Note that the G values from the right body side were not used in the prediction, as visual inspection of the EMG records suggested that the EMG magnitudes of the right and left body sides could differ. R^2 values were again calculated to assess whether the fits for the left body side (validation) were significantly worse than for the right body side (optimization).

2.6. Statistical analysis

In our experimental design, between-muscle comparisons are not meaningful, since each muscle is tested for its own unique directions; however, between-direction comparisons within a muscle are meaningful as they address the question of whether a muscle's response varies with the direction of perturbation. The effect of direction on the velocity onset time and on each muscle's EMG onset time, R^2, r_D, and r_A was examined using a one-way repeated-measures analysis of variance (ANOVA). Differences between the *PDA model* and *PD model*, and between the left and right body sides, were tested, for each muscle, using a one-tailed, paired repeated-measures t-test. Significance was set at $p < 0.05$ for all tests. All dependent variables obeyed a normal distribution, as tested by the Kolmogorov-Smirnov test [29]. Parameter values are presented using their mean and standard deviation.

3. Results

3.1. Discarded ensembles

In line with our expectations, all muscles had perturbation directions for which their response was absent or inconsistent. As such, only data from the three perturbation directions for which a muscle's EMG amplitudes were greatest were retained for that muscle. Overall, directions 4, 5, and 6 were retained for the right RA and EO, directions 5, 6, and 7 for the right IO, and directions 8, 1, and 2 for the right T9 and L3. However, since, for T9 and L3 in direction 2, some participants showed an increase in EMG amplitude over baseline while others showed a decrease or no change, this direction was omitted. We refer to the retained directions as each muscle's "principal directions".

For some retained ensembles, fits were poor, which was defined as having an R^2 of less than 0.5. For these ensembles, the R^2 values and the onset times were retained, but the ratios r_D and r_A were not. All data for one participant who consistently did not return to upright within 3 s of perturbation onset were also discarded. In some trials, visual inspection of the motion suggested that the trunk did not behave as a single rigid segment. In these trials, the distance between the LV3 and CV6 markers often varied within the trial due to twisting or lateral bending of the spine. For this reason, trials in which the linear distance between these two markers varied by more than 2 cm were deemed to be overly affected by trunk non-rigidity, and were discarded. Only ensembles with at least three good trials were retained.

3.2. Muscle response profiles and EMG onset times

Fig. 2 depicts EMG levels for the right muscles (top plot) as well as the trunk kinematics and perturbation force (bottom plot) from a representative ensemble of one participant for a forward perturbation (direction 1). Several features were consistent across muscles and perturbation directions: EMG levels as well as trunk acceleration and velocity were largest during the perturbation. Outward motion was comparatively rapid, whereas the return to upright was more gradual. EMG levels of the muscles that opposed the outward motion (T9 and L3 in Fig. 2) were largest, whereas those of their antagonists (RA in Fig. 2) remained near baseline. EMG profiles were most correlated with trunk velocity, but varied with all three kinematic variables. All EMGs returned to baseline levels (or below) at a time when the trunk was still travelling inward.

Fig. 3 shows the average, across-participant EMG profiles for all muscles and their respective principal directions. For all muscles, EMG magnitudes followed the same general time course. After an EMG onset time of approximately 200 ms, the EMG rose rapidly to its peak approximately 200 ms later, then slowly declined back towards baseline levels. Baseline levels were reached at approximately the same time as the peak inward velocity (not shown), i.e., well before the trunk reached the vertical. As can be seen in Fig. 4, average, across-participant EMG onset times were lowest for EO (127 ± 59 ms) and largest for T9 (231 ± 65 ms). Only those for RA varied significantly with direction ($p = 0.006$). Average,

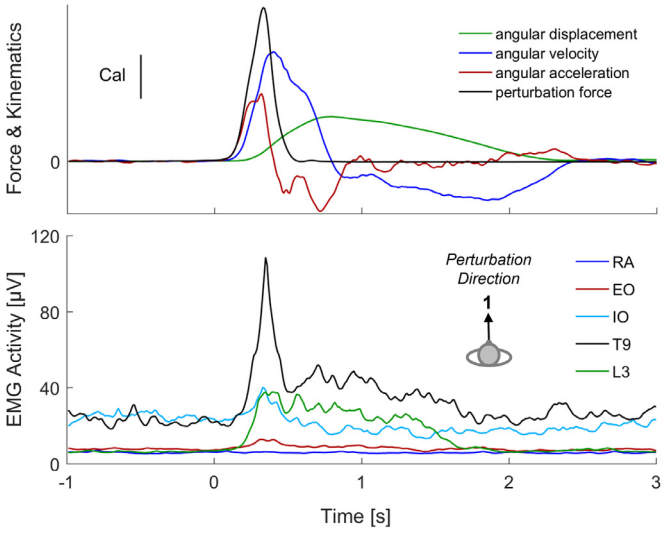

Fig. 2. A typical ensemble from one participant (average of 5 trials), showing the force for a forward perturbation (direction 1), kinematics, and EMG from all five muscles of the right trunk side: rectus abdominis (RA); external obliques (EO); internal obliques (IO); and erector spinae at the level of the ninth thoracic vertebra (T9) and the third lumbar vertebra (L3). Time of 0 s represents the perturbation onset. Calibration bar: 21 deg, 23 deg/s, 210 deg/s^2, and 59 N.

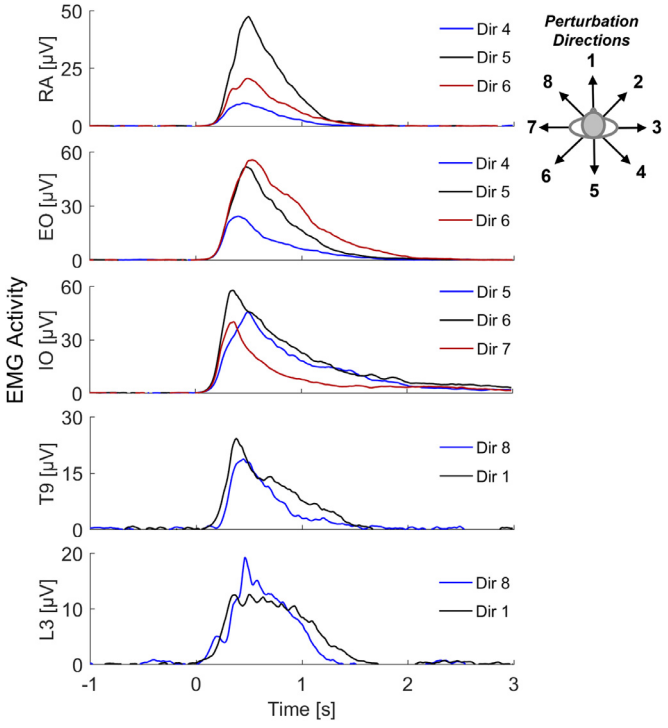

Fig. 3. Average, across-participant EMG profiles for all five right-side muscles and their principal directions. Muscles are: rectus abdominis (RA); external obliques (EO); internal obliques (IO); and erector spinae at the level of the ninth thoracic vertebra (T9) and the third lumbar vertebra (L3). Averaging across participants resulted in EMG peaks that were smoother and broader than those seen in individual participants (e.g., Fig. 2). Time of 0 s represents the perturbation onset.

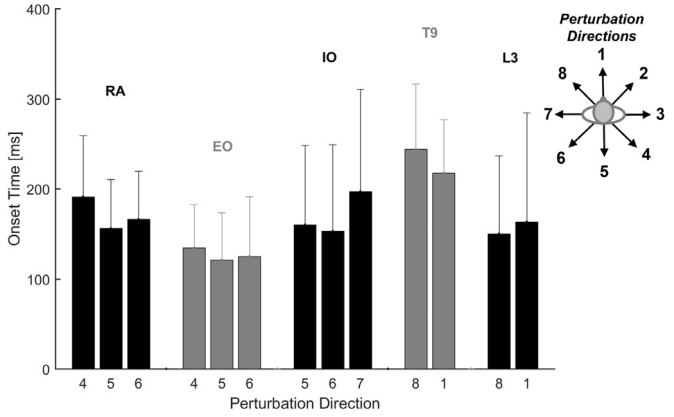

Fig. 4. Average, across-participant EMG onset times (mean and one standard deviation) for all five right-side muscles and their principal directions. Muscles are: rectus abdominis (RA); external obliques (EO); internal obliques (IO); and erector spinae at the level of the ninth thoracic vertebra (T9) and the third lumbar vertebra (L3). Numbers below the bars indicate the perturbation directions.

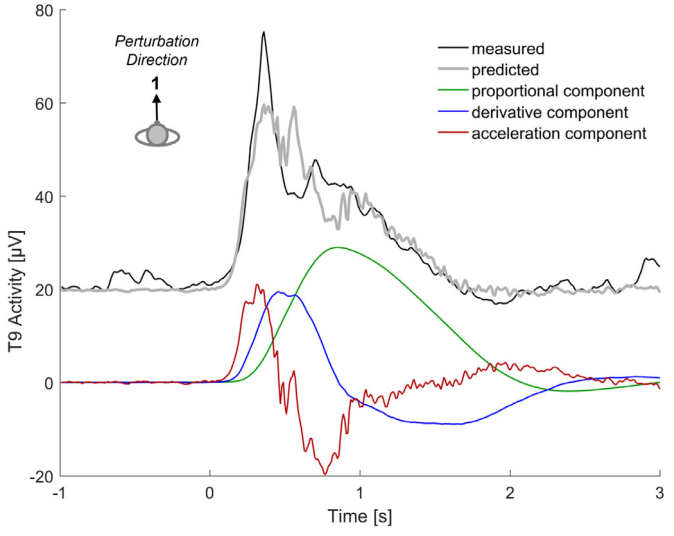

Fig. 5. Exemplary decomposition of the predicted EMG profile into its position-, velocity-, and acceleration-dependent components for one 5-trial ensemble. Shown are, for the erector spinae at the level of the ninth thoracic vertebra (T9) and a forward perturbation (direction 1): the measured EMG; the predicted EMG; and the EMG component due to trunk displacement (proportional component), trunk velocity (derivative component), and trunk acceleration (acceleration component). Time of 0 s represents the perturbation onset.

across-participant velocity onset times were 110 ± 11 ms and did not vary with direction ($p = 0.660$).

3.3. Model parameter estimation

Our hypothesis, i.e., that EMG amplitude correlates with trunk kinematics, proved to be true, with some exceptions. An example of the prediction using the *PDA model* is shown in Fig. 5 (T9, direction 1). Fits were generally good, with average, across-participant R^2 values varying between 0.68 and 0.92, depending on the muscle and direction (Fig. 6A). As can be seen in Fig. 5 and from the average, across-participant ratios r_D and r_A in Figs. 6B and C, all three gains, K_P, K_D, and K_A, were needed to produce the best fits.[1]

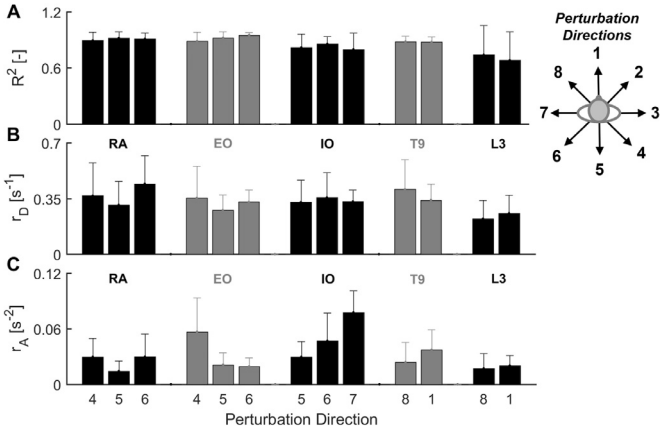

Fig. 6. Average, across-participant values (mean and one standard deviation) for the coefficient of determination, R^2 (A), ratio r_D (B), and ratio r_A (C) for the *PDA model*, in dependence of muscle and perturbation direction. Muscles are: rectus abdominis (RA); external obliques (EO); internal obliques (IO); and erector spinae at the level of the ninth thoracic vertebra (T9) and the third lumbar vertebra (L3). Numbers below the bottom plot indicate the perturbation directions.

The R^2 values for the *PD model* were significantly lower than those for the *PDA model*, with mean differences in R^2 ranging from 0.05 to 0.2 ($0.000 < p < 0.047$) depending on the muscle. Fig. 5 suggests that the main contribution of the acceleration component was to capture the rapid initial rise of the EMG.

Given that balance perturbations can presumably occur in any direction, it was important to examine whether fits and parameter values depended on the perturbation direction. As can be seen in Fig. 6, the observed variations in R^2, r_D, and r_A depended on both muscle and direction. Fit quality, as measured with R^2, varied significantly with direction for EO only ($p = 0.036$). Ratio r_D varied significantly with direction for RA only ($p < 0.001$), and ratio r_A for EO and IO only (both $p < 0.001$). This implies that perturbation direction only affected fits and parameter values in a few conditions.

When using the identified K_P, K_D, and K_A gains from the right-side muscles to predict the corresponding EMG for the left-side muscles in each participant, it was found that R^2 was significantly lower for RA, EO, and IO only. Mean differences in R^2 ranged from 0 to 0.1. This suggests that the model is valid for an independent dataset that is obtained using the same experimental paradigm.

4. Discussion

This study set out to use trunk kinematics to predict the EMG response of the major trunk muscles when the trunk is exposed to transient mechanical perturbations during sitting. In what follows, we characterize the muscle response predictions and discuss their implications for the development of closed-loop FES technology.

4.1. Kinematics-based prediction of muscle response

Our results show that the muscle response can be predicted using a simple linear, time-invariant combination of trunk angle, angular trunk velocity, and angular trunk acceleration. This prediction was similarly good for the principal directions of all muscles examined. To our knowledge, this is the first study to propose a model that can predict the full time course of the trunk muscle response from trunk kinematics, and this for all muscles and perturbation directions. Our model has the advantage of predicting

[1] A sporadic investigation showed that the results for the model ratios r_D and r_A, the muscle activity predictions, and the fit R^2 were largely unaffected by: (1) filtering the EMG data at a different cut-off frequency; (2) using a different vector for approximating tilt angle of the trunk; and (3) using a different differentiation scheme for obtaining trunk velocity and acceleration (see Section 2.3.). Details on the processing choices and the robustness of the associated results can be found in Supplementary Material S1.

the entire response, from perturbation initiation to recovery of upright position.

The finding that the *PDA model* provided good fits without a delay term was initially surprising, especially since EMG levels remained at or near baseline levels for up to 200 ms after perturbation onset. Lockhart and Ting [27] have also reported that a *PDA model* provided best fits without a delay term, even though an obvious delay was present. We attribute the finding of zero delay to the fact that, in our study, EMG activity first lags, then is in phase with, and finally leads trunk velocity, which was most correlated with the EMG profiles (see Fig. 2). While this overall temporal relation suggests an average lead or lag that is close to zero, the timing of trunk angle and trunk acceleration must contribute to this finding as well.

The EMG profiles resembled the output of a closed-loop, negative feedback control system that utilizes trunk kinematics as feedback information. This resemblance could be caused by several neural pathways including the stretch reflex, long-latency reflexes, and vestibular responses [14,15,30]. Because the movement lasts longer than voluntary reaction times, a voluntary component may also be present, i.e., the participants may be consciously using sensory information to guide the return to the vertical position. Feedback control has been observed in many other human voluntary movements [31]. For example, the EMG of the erector spinae muscles is known to increase with angle from the vertical during static leaning tasks, in response to the torque created by the weight of the trunk [32].

The parameters r_D and r_A reflect the relative importance of trunk velocity versus trunk acceleration in predicting the measured EMG profiles. The fact that r_D was about 10 times larger than r_A for all muscles (Fig. 6) suggests that angular trunk velocity is more relevant than angular trunk acceleration in determining muscle activity. For most muscles, r_D and r_A – and consequently the relative gains, or weights, of the kinematic variables – did not vary with direction (Fig. 6). Thus, the nervous system could be simplifying the task of remaining upright by using the same gains for a given muscle regardless of both direction and time, as has been suggested for standing balance [27]. However, since direction significantly affected r_D for one muscle (RA) and r_A for two muscles (EO and IO), this interpretation may not be true for all muscles.

Ting and her colleagues have proposed a theory of standing balance [27,33] that could also explain the main results of this study. It states that the CNS integrates the various sensory inputs available to it to form an internal representation of the position, velocity, and acceleration of the body's center of mass. The CNS then chooses direction-independent feedback gains on the kinematics that will lead to muscle activation levels and profiles restoring the center of mass' original position. This explanation has been used to explain the control of standing balance in humans and cats, but has not been applied to the control of seated balance. Assuming that the trunk behaves approximately like a rigid body [1,16], the angular trunk kinematics in the present study would be proportional to the motion of the upper body's center of mass, implying that the proposed theory could apply to our results as well.

4.2. Implications for FES control of sitting posture

Our findings have implications for the design of an FES system for real-time, feedback-based control of seated posture. Based on recent findings demonstrating that a physiologically inspired FES control strategy improves trunk stability more effectively than co-contractions [24], we assume that phasic muscle stimulation that mimics the EMG response of non-disabled individuals is desirable. Further arguments for this rationale may include that control mimicking natural patterns may: (1) be more easily mastered by the user; (2) result in movement that appears natural; and (3) mesh more easily with any residual voluntary control the user has retained. However, arguments against mimicking non-disabled behavior are valid as well, e.g., when taking advantage of novel control approaches to stabilize posture [34].

For the perturbations used here, our results suggest that all of the CNS-controlled mechanisms to counter the perturbation would be close-to-absent following complete SCI. This is consistent with everyday experience, and with the observation that spinalized cats can stand up, but cannot resist balance perturbations [35]. Without baseline activation, intrinsic muscle stiffness will be ineffective, and without long-latency and voluntary inputs, there will be little EMG response. However, individuals with complete SCI may be able to withstand small, more impulsive perturbations that elicit a large EMG response in the back extensor muscles approximately 30 ms following perturbation onset [36]. Since Ia pathways below the injury are preserved and potentially hyperactive after spinal cord injury [37], the stretch reflex, whose amplitude increases with velocity of stretch [38], may be used to resist movement.

As can be seen in Fig. 2, the last phase of returning to upright posture is accomplished without active muscle engagement. As such, the overall strategy of the CNS appears to be to use muscle contractions to "brake" the perturbation-induced trunk displacement and "launch" the trunk back towards the vertical, but then use the trunk's momentum without muscle contractions to reach upright sitting posture. We speculate that this strategy may reduce muscle fatigue. Given that muscle fatigue is one of the top challenges when using FES, implementing a similar strategy when using closed-loop FES control to stabilize dynamic sitting posture may be beneficial.

For the first 200 ms following perturbation onset, the main torque acting to slow outward motion is due to: (1) mechanisms intrinsic to passive control [3–8] (*see Introduction*) and (2) baseline muscle co-contractions that are present during upright sitting to enhance overall trunk stiffness [2]. Thus, baseline stimulation of paralyzed muscles may be needed to enhance trunk stiffness for the purpose of stabilizing upright sitting, but to also support effective recovery from a perturbation. In the context of designing a practical FES system, we have already demonstrated that trunk stiffness during upright sitting can be increased via a *continuous FES control component* that co-contracts the muscles using low-intensity, open-loop electrical stimulation [18]. The present work therefore takes the first step towards an additional, *intermittent FES control component* that applies kinematics-based, closed-loop stimulation to stabilize the body against motion in the sagittal and frontal planes due to transient perturbations. Such intermittent FES component can then be paired with low-intensity, open-loop FES [18] to facilitate stability during quiet sitting and transient perturbations.

Since R^2 for the *PDA model* was larger than 0.68 for all muscles, the same model type (*PDA model*) can be used to regulate the stimulation profiles for all muscles and directions, potentially simplifying controller design. However, different muscles may require different gains, with three muscles, RA, EO, and IO, requiring feedback gains that vary with direction.

Two studies that have used FES to enhance trunk stability during sitting applied linear feedback controllers based on trunk kinematics. Vanoncini et al. [16] used a proportional-integral-derivative controller with no time delay, augmented with a simple inverted pendulum model of the upper body, to stimulate the back extensors in one individual with SCI. This approach was evaluated for voluntary movement as well as light perturbations in the sagittal plane. Audu et al. [19] achieved good results when using a proportional-derivative controller with no time delay to stimulate the hip and trunk extensor muscles in response to a forward perturbation. Also our findings suggest that a *PD model* is likely to be a good choice; adding an acceleration feedback term

to the model may, however, yield a better performance: it will cause the stimulation to begin sooner, which may be desirable for rapidly braking outward travel.

4.3. Limitations

The performed work has several limitations. First, we have shown for only one particular type of perturbation that Eq. (1) provides good fits; as such, the results need to be confirmed with other types of perturbations causing different trunk kinematics. Second, we eliminated trials that were characterized by a non-rigid trunk. Modeling efforts need to be extended to such behavior as well, especially if they are to be applied to trunk control following SCI. Third, we restricted our analysis to the principal directions of each muscle. This may, however, not be a major limitation for an FES system, since it may not be necessary to stimulate all muscles in all directions, potentially also reducing muscle fatigue. Fourth, we observed slight variations in perturbation magnitudes with perturbation direction [26], which may have affected the reported parameter variations; however, other work with more uniform perturbations [9] has shown that EMG levels do, in fact, vary with direction. Fifth, it needs to be acknowledged that deep muscles of the abdominal cavity (e.g., iliopsoas, quadratus lumborum) and the muscles crossing the hip (e.g., rectus femoris, biceps femoris, obturator externus, glutei, sartorius) contribute to pelvic stability during sitting. Therefore, future work should investigate whether kinematics-based models of muscle activity prediction can be established for these muscles as well. Finally, the current results do not allow us to determine the relative importance of each muscle's contribution to the stabilization act. In an actual FES system, the muscles' relative contribution could be explored by investigating the kinematic effect of keeping select muscles unstimulated, one at a time.

In the context of designing a practical FES system, the described approach of combining continuous, open-loop FES with intermittent, closed-loop FES implies that the outcomes of this study cannot be used on their own to stabilize the upper body during sitting. Rather, they are the basis for the FES control component that provides intermittent control against transient perturbations using kinematic information. Future work is needed to examine whether the two FES control components can, when combined, facilitate upright stability during both quiet sitting and transient perturbations. Additional FES control components may be needed to also account for quasi-static situations requiring more substantial co-contractions, e.g., in a prolonged forward leaning position.

Acknowledgements

We would also like to thank Vivian Sin for her contributions to experimental data acquisition and processing.

Competing Interests

There are no conflicts of interest for the authors of this study.

Funding

This study was funded through a Discovery Grant from the Natural Sciences and Engineering Research Council of Canada (RGPIN-2014-04666).

Ethical Approval

The experimental procedures of this study were approved by the research ethics boards of the University of Toronto, Toronto, Canada (Study ID: #15699) and the Toronto Rehabilitation Institute, Toronto, Canada (Study ID: #05-017).

Supplementary materials

Supplementary material associated with this article can be found, in the online version, at doi:10.1016/j.medengphy.2018.05.004.

References

[1] Audu ML, Triolo RJ. Intrinsic and extrinsic contributions to seated balance in the sagittal and coronal planes: implications for trunk control after spinal cord injury. J Appl Biomech 2015;31(4):221–8.
[2] Masani K, Sin VW, Vette AH, Thrasher TA, Kawashima N, Morris A, et al. Postural reactions of the trunk muscles to multi-directional perturbations in sitting. Clin Biomech 2009;24(2):176–82.
[3] White AA, Panjabi MM. Clinical biomechanics of the spine. 2nd ed. Philadelphia: Lippincott Williams & Wilkins; 1990. Chapters 1–2.
[4] Panjabi MM, Brand RA, White AA. Three-dimensional flexibility and stiffness properties of the human thoracic spine. J Biomech 1976;9:185–92.
[5] Gardner-Morse MG, Stokes IAF. Structural behavior of human lumbar spinal motion segments. J Biomech 2004;37:205–12.
[6] Vette AH, Masani K, Wu N, Popovic MR. Multidirectional quantification of trunk stiffness and damping during unloaded natural sitting. Med Eng Phys 2014;36(1):102–9.
[7] Gardner-Morse MG, Stokes IAF. Trunk stiffness increases with steady-state effort. J Biomech 2001;34:457–63.
[8] Cholewicki J, Juluru K, McGill SM. Intra-abdominal pressure mechanism for stabilizing the lumbar spine. J Biomech 1999;32:13–17.
[9] Preuss R, Fung J. Musculature and biomechanics of the trunk in the maintenance of upright posture. J Electromyogr Kinesiol 2008;18(5):815–28.
[10] Zedka M, Kumar S, Narayan Y. Electromyographic response of the trunk muscles to postural perturbation in sitting subjects. J Electromyogr Kinesiol 1998;8(1):3–10.
[11] McGill SM, Grenier S, Kavcic N, Cholewicki J. Coordination of muscle activity to assure stability of the lumbar spine. J Electromyogr Kinesiol 2003;13(4):353–9.
[12] Milosevic M, Valter McConville KM, Sejdic E, Masani K, Kyan MJ, Popovic MR. Visualization of trunk muscle synergies during sitting perturbations using self-organizing maps (SOM). IEEE Trans Biomed Eng 2012;59(9):2516–23.
[13] Stokes IA, Gardner-Morse M. Lumbar spinal muscle activation synergies predicted by multi-criteria cost function. J Biomech 2001;34(6):733–40.
[14] Goodworth AD, Peterka RJ. Contribution of sensorimotor integration to spinal stabilization in humans. J Neurophysiol 2009;102(1):496–512.
[15] Goodworth AD, Peterka RJ. Influence of bilateral vestibular loss on spinal stabilization in humans. J Neurophysiol 2010;103(4):1978–87.
[16] Vanoncini M, Holderbaum W, Andrews BJ. Electrical Stimulation for trunk control in paraplegia: a feasibility study. Control Eng Pract 2012;20(12):1247–58.
[17] Ho CH, Triolo RJ, Elias AL, Kilgore KL, DiMarco AF, Bogie K, et al. Functional electrical stimulation and spinal cord injury. Phys Med Rehabil Clin N Am 2014;25(3):631–54.
[18] Vette AH, Wu N, Masani K, Popovic MR. Low-intensity functional electrical stimulation can increase multidirectional trunk stiffness in able-bodied individuals during sitting. Med Eng Phys 2015;37(8):777–82.
[19] Audu ML, Lombardo LM, Schnellenberger JR, Foglyano KM, Miller ME, Triolo RJ. A neuroprosthesis for control of seated balance after spinal cord injury. J Neuroeng Rehabil 2015;12(1):8.
[20] Triolo RJ, Bailey SN, Lombardo LM, Miller ME, Foglyano K, Audu ML. Effects of intramuscular trunk stimulation on manual wheelchair propulsion mechanics in 6 subjects with spinal cord injury. Arch Phys Med Rehabil 2013;94(10):1997–2005.
[21] Triolo RJ, Bailey SN, Miller ME, Lombardo LM, Audu ML. Effects of stimulating hip and trunk muscles on seated stability, posture, and reach after spinal cord injury. Arch Phys Med Rehabil 2013;94(9):1766–75.
[22] Wilkenfeld AJ, Audu ML, Triolo RJ. Feasibility of functional electrical stimulation for control of seated posture after spinal cord injury: a simulation study. J Rehabil Res Dev 2006;43(2):139–52.
[23] Lambrecht JM, Audu ML, Triolo RJ, Kirsch RF. Musculoskeletal model of trunk and hips for development of seated-posture-control neuroprosthesis. J Rehabil Res Dev 2009;46(4):515–28.
[24] Patel K, Milosevic M, Nakazawa K, Popovic MR, Masani K. Wheelchair neuroprosthesis for improving dynamic trunk stability. IEEE Trans Neural Sys Rehab Eng 2017;25(12):2472–9.
[25] Murphy JO, Audu ML, Lombardo LM, Foglyano KM, Triolo RJ. Feasibility of closed-loop controller for righting seated posture after spinal cord injury. J Rehabil Res Dev 2014;51(5):747–60.
[26] Thrasher TA, Sin VW, Masani K, Vette AH, Craven BC, Popovic MR. Responses of the trunk to multidirectional perturbations during unsupported sitting in normal adults. J Appl Biomech 2010;26(3):332–40.
[27] Lockhart DB, Ting LH. Optimal sensorimotor transformations for balance. Nat Neurosci 2007;10(10):1329–36.
[28] Glantz SA, Slinker BK. Primer of applied regression and analysis of variance. 1st ed. New York: McGraw-Hill, Health Professions Division; 1990.
[29] Press WH, Vetterling WT. Numerical recipes. Cambridge: Cambridge University Press; 1989.

[30] Deliagina TG, Beloozerova IN, Orlovsky GN, Zelenin PV. Contribution of supraspinal systems to generation of automatic postural responses. Front Integr Neurosci 2014;8:76.
[31] Scott SH, Cluff T, Lowrey CR, Takei T. Feedback control during voluntary motor actions. Curr Opin Neurobiol 2015;33:85–94.
[32] Floyd WF, Silver PHS. Function of erectores spinae in flexion of the trunk. Lancet 1951;1(6647):133–4.
[33] Welch TDJ, Ting LH. A feedback model reproduces muscle activity during human postural responses to support-surface translations. J Neurophysiol 2008;99(2):1032–8.
[34] Jovic J, Bonnet V, Fattal C, Fraisse P, Coste CA. A new 3D center of mass control approach for FES-assisted standing: first experimental evaluation with a humanoid robot. Med Eng Phys 2016;38(11):1270–8.
[35] Macpherson JM, Fung J. Weight support and balance during perturbed stance in the chronic spinal cat. J Neurophysiol 1999;82(6):3066–81.
[36] Granata KP, Slota GP, Bennett BC. Paraspinal muscle reflex dynamics. J Biomech 2004;37(2):241–7.
[37] Mirbagheri M, Barbeau H, Ladouceur M, Kearney R. Intrinsic and reflex stiffness in normal and spastic, spinal cord injured subjects. Exp Brain Res 2001;141:446–59.
[38] Kearney RE, Stein RB, Parameswaran L. Identification of intrinsic and reflex contributions to human ankle stiffness dynamics. IEEE Trans Biomed Eng 1997;44(6):493–504.